RADIAL CURRENT-DENSITY DISTRIBUTION IN THE MAIN SPOTS IN A PLASMA CUTTING ARC

Yu. Ya. Kiselev and V. K. Pogora

UDC 533.915.08:621.791.947.55

Measurements have been made on the current density in a cutting arc as affected by polarity and by the design and working parameters.

Air-plasma metal cutting is increasingly used, where the plasmotron may have a thermochemical cathode or a cylindrical copper electrode [1]. A major distinctive feature is that the arc burns between the inner electrode and the metal to be cut and passes through a narrow nozzle along with the air. Intense heating and rapid melting occur in the arc spot on the metal, while the plasma flux through the nozzle blows the molten metal away, and the spot moves along the generator in the cutting cavity.

The efficiency and economy in plasma cutting are dependent to a considerable extent on the heat transfer between the arc spot and the metal, and the rate of this is dependent on the spot parameters, particularly the radial current-density distribution.

Not much is known about that distribution in highly compressed cutting arcs. One can cite only [2], in which measurements were made only on anode spots of relatively uncompressed arcs, in the main with argon and nitrogen as gas.

The best method of measuring the spot current density is that based on a sectional electrode SE [3] (Fig. 1). The plasmotron P (Fig. 1a) is supplied from the power supply PS and is placed above the SE. The two sections in the electrode are insulated one from the other and cooled by water. When the electrode moves relative to the fixed plasmotron or vice versa, the arc spot passes from one section to the other. The projection of the spot on the chord AB (Fig. 1b) indicates the boundary electrically separating the two sections. The ammeter A measures the total arc current, while an oscilloscope records the current I(x) flowing through one section, which alters as the electrode moves (Fig. 1c).

The current through segment ABC when the chord AB is displaced by a distance x to the right of the arc axis (Fig. 1b) is

$$I(x) = 2\int_x^R j(r)\arccos\frac{x}{r}\,rdr. \tag{1}$$

We solve (1) for j(r):

$$j(r) = -\frac{1}{\pi}\int_r^R \frac{I''(x)\,dx}{\sqrt{x^2 - r^2}}. \tag{2}$$

Equation (2) is an inversion of an Abel integral equation. As I(x) is measured and the analytic expression is unknown, the radial distribution is derived by integrating (2) numerically in some way [4], which is considered in more detail below.

This method defines not the instantaneous density at some point in the anode or cathode spot and also not the sizes of the latter but instead some integral values at the electrode in the zone covered by the cathode or anode spots on prolonged arc running. Therefore, here we consider not the cathode or anode spots but the current spots on electrodes that may be anode or cathode.

The purpose of the study was to relate the density distributions in the main spots to the arc polarity, air flow, nozzle diameter, and distance of plasmotron from the metal.

Kishinev Polytechnical Institute. Translated from Inzhenerno-Fizicheskii Zhurnal, Vol. 53, No. 2, pp. 284-289, August, 1987. Original article submitted March 24, 1986.

 0022-0841/87/5302-0950$12.50

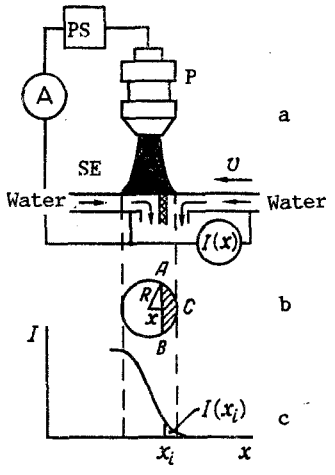

Fig. 1

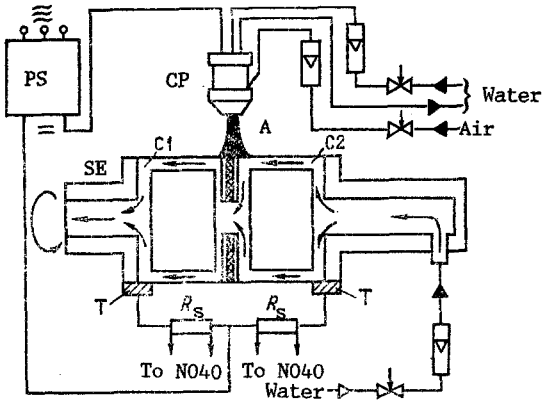

Fig. 2

Fig. 1. Illustration of the sectional-electrode method: a) block diagram; b) projection of main arc spot on electrode; c) curve for current in one of the electrode sections.

Fig. 2. Block diagram of apparatus for examining current density in cutting-arc spots: PS) power supply; CP) cutting plasmotron; A) cutting arc; SE) sectioned electrode; C1 and C2) electrode sections; T) current connections.

The apparatus (Fig. 2) consists of the cuttng plasmotron CP, the power supply PS, the sectional electrode SE, and appropriate control and measurement apparatus. The CP had an internal copper electrode and was built at the Lazo Kishinev Polytechnical Institute [1]. A choke force giving 500 V on open circuit provided the supply, which had a steeply falling voltage–current characteristic and provided smooth current control.

The plasma cutting arc has an extremely high thermal-energy concentration, and the heat flux at the metal is much more than 5×10^7 W/m^2, which is the limit for an immobile water-cooled copper electrode [5], so we used a rotating SE [2], which was made from two cylindrical copper sections between which there was an insulating insert of thickness 0.15×10^{-3} m. The sections were rigidly coupled together and cooled by water. The SE was rotated and the plasmotron was displaced along the rotation axis by means of a TV-4 lathe. The graphite brushes T brought the current to the sections. The series resistors R_s in the current circuits were connected to an NO40 light-beam oscillograph.

There were also instruments for controlling and measuring the air and water flows.

In all the experiments, the SE rotated at 75 rad/sec, while the plasmotron moved at 0.95×10^{-3} m/sec. Constant water flows were maintained in the plasmotron and SE: correspondingly 0.17 and 0.15 kg/sec. The working current was 100 A.

The following parameters were varied: air flow ($1.08 \cdot 10^{-3}$-$1.42 \cdot 10^{-3}$ kg/sec), distance between plasmotron and electrode (10^{-2}-$2 \cdot 10^{-2}$ m), and nozzle diameter ($2.7 \cdot 10^{-3}$-$4 \cdot 10^{-3}$ m). In every case, forward and reversed polarities were used.

The working arc was initially struck on one of the sections far from the boundary. Then when the required state had been attained, the displacement mechanism and oscillograph were activated. The oscillograms were considered suitable if there were no sharp current shifts and the curves were symmetrical about the point representing equal currents in the sections.

The spot diameter was taken as the distance on the oscillogram on an appropriate scale at which the current in one section had altered from the value equal to the total current to the threshold.

I(x) was differentiated graphically and (2) was solved numerically by the method of [6]; the resulting j(r) is sensitive to input data errors, so the accuracy was improved by using enlarged oscillograms, while the recorded I(x) was smoothed by least squares. Each measured $I(x_i)$ was replaced by a mean $\overline{I(x_i)}$, which was derived from six points symmetrically disposed about x_i, which were fitted to a polynomial of third degree [7].

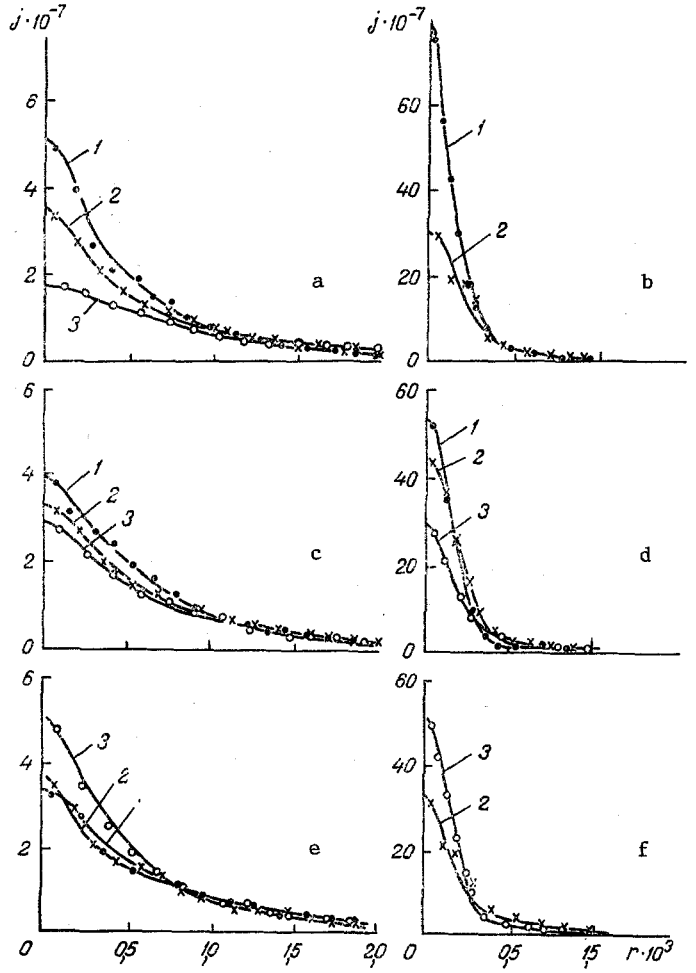

Fig. 3. Radial density distributions with forward polarity (a, c, and e) and reverse polarity (b, d, and f): a and b) $d = 3.4 \cdot 10^{-3}$ m; $G = 1.25 \cdot 10^{-3}$ kg/sec, h in 10^{-3} m: 1) 10; 2) 15; 3) 20; c and d) $h = 15 \cdot 10^{-3}$ m; $G = 1.08 \cdot 10^{-3}$ kg/sec, d in 10^{-3} m: 1) 2.7; 2) 3.4; 3) 4.0; e and f) $d = 3.4 \cdot 10^{-3}$ m; $h = 15 \cdot 10^{-3}$ m; G, 10^{-3} kg/sec: 1) 1.08; 2) 1.25; 3) 1.42. j, A/m²; r, m.

The current density at a point is [6]

$$j_k = -\frac{2}{\pi b} \sum_{n=k}^{N} B_{k,n} I'_n. \tag{3}$$

Calculations were performed on j(r) for N = 10, 20, 30, 40, and 60 in order to establish the optimum number of zones; the result was found as N = 30 on the basis of the subsequent calculations. The arc current was also checked from the densities in each of the zones, where the difference between the calculated and measured values was not more than 4%. An SM-3 computer was used.

When the distance from the end of the nozzle to the SE was increased from 10^{-2} to 2×10^{-2} m with direct polarity (Fig. 3a, SE the anode), the density at the center decreased from 5×10^7 to 1.7×10^7 A/m², while the spot diameter increased from 3.6×10^{-3} to 4.7 10^{-3} m. With reverse polarity (Fig. 3b, SE the cathode), increase from 10^{-2} to 1.5×10^{-2} m reduced the central density from 72×10^7 to 30×10^7 A/m², while the diameter increased from 1.3×10^{-3} to 2.1×10^{-3} m.

Similar regularities occurred on increasing the nozzle diameter; e.g., between 2.7×10^{-3} and 4×10^{-3} m with direct polarity (Fig. 3c) there was a reduction in the central density from 3.9×10^7 to 2.9×10^7 A/m², diameter increasing from 3.6×10^{-3} to 5.1×10^{-3} m, while with reverse polarity (Fig. 3d), the corresponding changes were $54 \cdot 10^7$-$29 \cdot 10^7$ A/m² and $1.8 \cdot 10^{-3}$-$2.5 \cdot 10^{-3}$ m.

The density and diameter varied in a more complicated way with the air flow (Fig. 3e and f).

The results are:

1) the density is described by

$$j(r) = j_{max} \exp(-Kr^2); \quad (4)$$

2) the central density with reverse polarity is higher by more than an order of magnitude than that with direct; and

3) the diameter with reverse polarity is about half that with direct.

NOTATION

I(x), measured current change in one electrode section; x, coordinate; R, radius of current spot on electrode; j(r), current density at distance r from axis of arc ($0 \leq r \leq R$); I"(x), second derivative of I(x); R_s, series resistance; $I(x_i)$, value of I(x) at point x_i; j_k, current density in zone k, k = 1, ..., N; N, number of division zones in spot radius; b, width of division zone; $B_{k,n}$, constant coefficients [6]; I'_n, derivative of I(x) at point n on spot radius; d, nozzle diameter; G, air flow; h, distance from plasmotron to sectioned electrode; j_{max}, current density at spot center; $K = j_{max}/j_{av}$, current localization factor.

LITERATURE CITED

1. Yu. Ya. Kiselev, Air-Plasma Metal Cutting with Copper Electrodes [in Russian], Kishinev (1977).
2. S. P. Polyakov and P. F. Bulanyi, Fiz. Khim. Obrab. Mater., No. 6, 137-139 (1980).
3. P. A. Shoek, Modern Heat-Transfer Problems [in Russian], Moscow–Leningrad (1966), pp. 110-116.
4. L. T. Lar'kina and V. S. Éngel'sht, Reduction to a Homogeneous Optically Thin Layer in Axisymmetric Objects [in Russian], Dep. VINITI No. 6917-73, Frunze (1973).
5. M. F. Zhukov, A. S. Koroteev, and B. A. Uryukov, The Applied Dynamics of Thermal Plasmas [in Russian], Novosibirsk (1975).
6. O. N. Nestor and H. N. Olsen, SIAM Rev., 2, No. 3, 200-207 (1960).
7. K. Bockasten, JOSA, 51, No. 9, 943 (1961).